

The role of source modeling in prestack depth migration for AVO estimation

Saul E. Guevara and Gary F. Margrave

ABSTRACT

A progress report on the true amplitude migration issue for AVO is presented here. Synthetic seismic data are generated using elastic Finite Difference modeling, and PreStack Depth Migration is carried out on these data using the PSPI approach. Angle gathers of the migrated data are generated, and its amplitude versus angle relationship is compared to the theoretical amplitudes from the Zoeppritz equations. The source is modeled using a 2-D Green's function solution. Characteristics of the migrated data for PP and PS wave modes, including postcritical events, are analyzed. Some explanations are proposed and issues for future research in this topic are raised.

INTRODUCTION

Migration has shown good results on obtaining information from the geology, especially related to the geometry. However, to obtain more details related to lithology, is required true amplitude recovery. AVO is an example of such a method. Some authors have studied the relation between amplitude and migration, and many different approaches can be identified, each one with its specific approximations (e.g. Gray 1997). However real true amplitude probably is not too close to be obtained.

In principle, according to Claerbout (1971), "reflectors exist at points in the ground where the first arrival of the downgoing wave is time coincident with an upgoing wave". Wave equation migration, as proposed by Claerbout (1971), requires two steps: downward propagation and imaging condition. This definition assumes the summation of amplitudes for an specific location to obtain the image. In the case of shot-profile migration, where a common shot gather is migrated, the downgoing wave corresponds to a source model and the upgoing to the recorded data. Hence the model of the source can contribute enhance or disturb the resulting reflectivity.

The Pre stack depth migration approach known as wave equation migration (WEM), is based on a one-way approximation to the wave equation propagation.. Some authors have considered the amplitudes and source modeling issues for one-way propagator migration. Wapenaar (1990) states that the one-way source representation is not as simple as a delta function at zero time, and defines more appropriate equations (see also Al-Saleh et al, 2009). Besides that, as shown by Zhang et al. (2005), the one way wave equation operators, even when correct cinematically (propagation time) are not correct in amplitude, and a correction is proposed by them.

A study on the source representation is presented in this work. Synthetic seismic data are generated using elastic Finite Difference modeling, and PreStack Depth Migration is carried out on these data using the PSPI approach.

THEORY

Claerbout (1971) proposed the imaging condition as follows:

$$I(x, z) = \sum_{s_i} \int_{\omega} \frac{U(x, z; \omega)}{D(x, z; \omega)} d\omega$$

where $I(x, z)$ is the *image* at the location (x, z) , $U(x, z; \omega)$ corresponds to the Upgoing wave (data recorded), $D(x, z; \omega)$ to the Downgoing wave (source), both for the frequency component ω , and added together for all the sources s_i . This definition is good enough if only an image of the earth's geometry is required. But if we look for information of properties, we better talk about *reflectivity* instead of just *image*.

The PSPI approach (Gazdag and Sguazzero, 1984) is the one-way WEM method that was used in this work. The code was developed at CREWES and is described by Ferguson and Margrave (2005) and Al-Saleh et al. (2009). This method can be described by the following equation for the upgoing wavefield $U(x, \omega)$, after the equations presented by Al-Saleh, et al. (2009):

$$U_{n\Delta z}(x, \omega) = \frac{1}{2\pi} \int U_{(n-1)\Delta z}(x', \omega) dx' \int_{-\infty}^{\infty} \exp\left(i\sqrt{k^2 - k_x^2}\Delta z\right) \exp(-ik_x(x - x')) dk_x$$

where Δz is the depth step size and n is the number of the depth step, ω is the temporal frequency, k_x is the wavenumber in the direction x , and k is the magnitude of the wavenumber vector. An analogous expression can be defined for the downgoing wavefield.

The deconvolution imaging condition, following Margrave et al (2010) is:

$$I(x, z) = \int_{\omega} \frac{U(x, z, \omega)D^*(x, z, \omega)}{D(x, z; \omega)D^*(x, z, \omega) + \mu I_{max}(z)} d\omega$$

where the asterisk (*) means conjugate, and $\mu I_{max}(z)$ is a stabilizing factor.

The source implemented for this code is a numerical evaluation of the free-space Green's function at the first depth level below the source, which is a better representation than the extrapolation of an unit pulse, as shown by Al-Saleh et al. (2009), and in agreement with Wapenaar (1990).

As for true amplitude imaging, the following analysis, with the help of Green's Functions, shows that the source wave field at the reflector for a specular P-wave reflection, can be represented as

$$D(refl) = \frac{W(\omega)}{4\pi r_s} e^{ikr_s}$$

where $W(\omega)$ is the estimated wavelet, r_s is the distance to the surface, and k is the wavenumber. The data at the reflector is:

$$U(\text{refl}) = R_T \frac{W_T(\omega)}{4\pi r_s} e^{ikr_s}$$

where $W_T(\omega)$ corresponds to the true wavelet and R_T to the true reflectivity. Then the amplitude resulting from the deconvolution imaging condition would depend on the wavelet estimation, since:

$$R_D = R_T \frac{W_T(\omega)}{W(\omega)}$$

METHOD

The effect of the source on amplitude after migration was studied using synthetic data. Model data was generated with an elastic 2-D finite difference method. Two simple geological models were created to this purpose, with sources and receivers on a flat surface and with a horizontal reflecting interface. In both cases the geometry is the same: the thickness of the upper layer is 425 m and 500 m in second layer. The extension of the model is 2500 m, with the source located at 100 to the x-direction origin (Fig. 1a). This width allows to develop post-critical reflection events. As a source of energy we used a 30 Hz Ricker wavelet, which is a zero phase shifted wavelet, starting at time zero (Fig. 1b). It has a size of 0.066 s.

Tables 1 and 2 illustrate the parameters of each one of the geological models. The first model just include a common increase in velocity at the interface, and the second one was intended to correspond to a change of polarity for shorter incidence angles. Figure 2 illustrates the vertical and horizontal components after modeling for model 1. Events like surface waves, P-waves (the faster events) and S-waves can be identified. However, notice the strong leakage of two wave modes on both components for farther offsets.

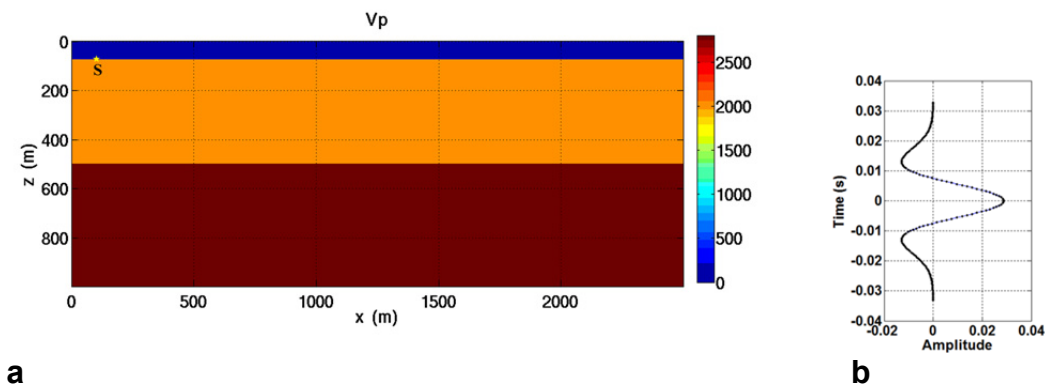


FIG. 1. (a) P-wave velocity of the geological model 1. (b) Wavelet used for modeling.

Layer	Vp (m/s)	Vs (m/s)	Density (Kg/m ³)
0	0	0	0
1	2000	1000	2000
2	2800	1600	2500

Table 1. Properties of the model 1.

Layer	Vp (m/s)	Vs (m/s)	Density (Kg/m ³)
0	0	0	0
1	3100	1500	2000
2	4000	2500	2020

Table 2. Properties of the model 2.

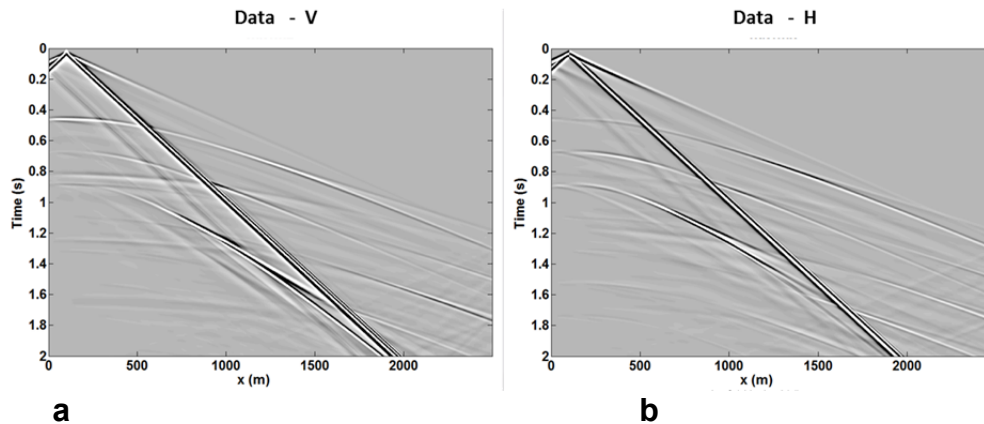


FIG. 2. Raw data for model 1. (a) Vertical component, (b) Horizontal component.

Prestack depth migration according to the PSPI approach was used, based on a code described by Ferguson and Margrave (2005) and Al-Saleh et al. (2009). Previously to migration the data was shifted by half of the wavelet time, such that the highest amplitude can correspond to the right depth. There was used a Green's function as the model for the source, displaced to the first depth step, as proposed by Al-Saleh et al. (2009). The vertical component was the input for the P wave migration and the horizontal for the Converted wave, assuming that they contain most of the corresponding energy. As for angle gathers definition, ray trace Matlab codes *traceray_pp* and *traceray_ps* were used.

CASE ANALYSIS

Results corresponding to the two geological models are presented in Figure 3 show the downward propagated source and data wavefields at the depth of the reflector, that is to say, the imaging condition. Fig. 3(b) correspond to the data of the PP wave and Fig. 3(c) to the PS wave. The arrival time agrees with the source time. However artifacts can be observed in the recorded data, especially for the PS wave.

Figure 4 shows modeling of the source using finite difference, which was obtained with the receivers on the reflector. Comparing with Fig. 1(a), phase variations can be observed in the migration source and not in modeling.

Figure 5 shows the migrated gathers in the angle domain. One might expect a continuous line at the reflector depth, however, the line becomes blurry after about 25° for PP and after about 40° for PS data. Finally, Fig. 6 shows the comparison of amplitudes between PP and PS, and their corresponding theoretical Zoeppritz solution. A scale factor was required in this case, to obtain comparable amplitudes. There is reasonable resemblance for shorter angles lower than the critical angle. For higher angles the energy is too low.

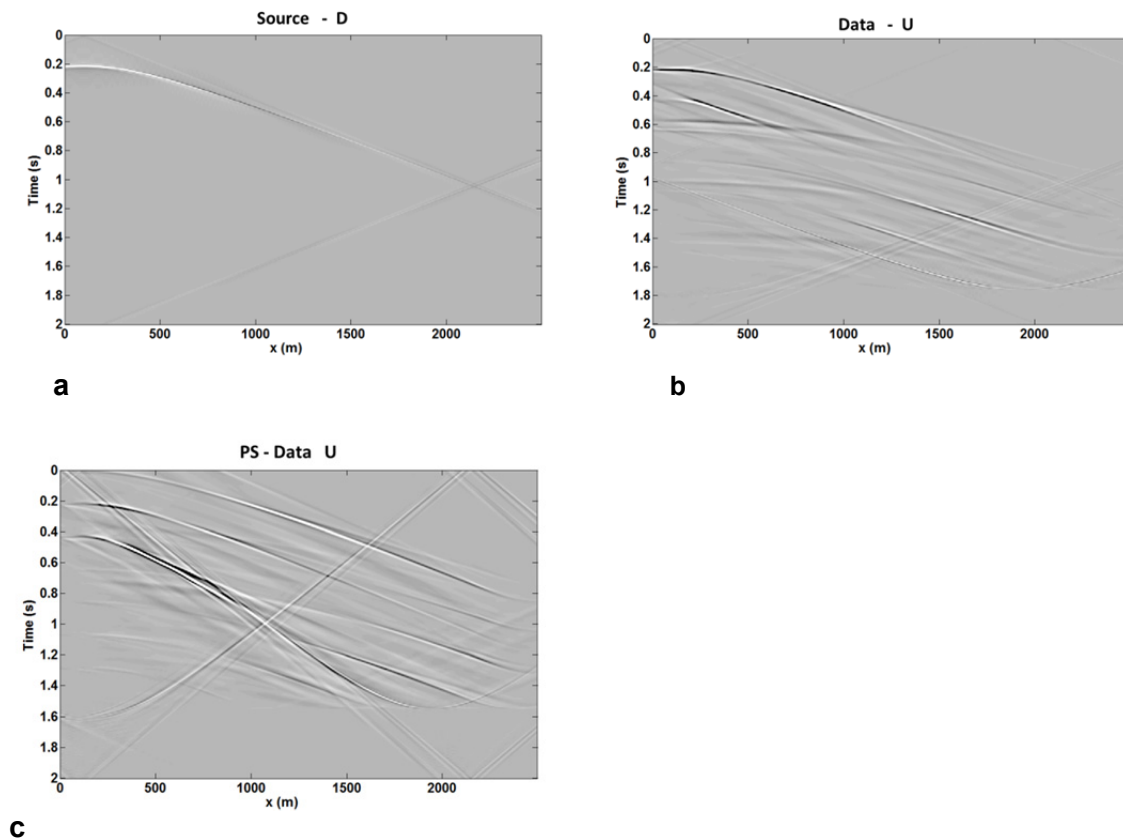


FIG. 3. Downward propagated source (D) and data (U) wavefields for migrations of the geological Model 1 at the depth corresponding to the reflector. (a) The source wavefield, (b) the P-wave data (vertical component) for the PP migration, (c) the S-wave data (Horizontal component) for the PS-migration.

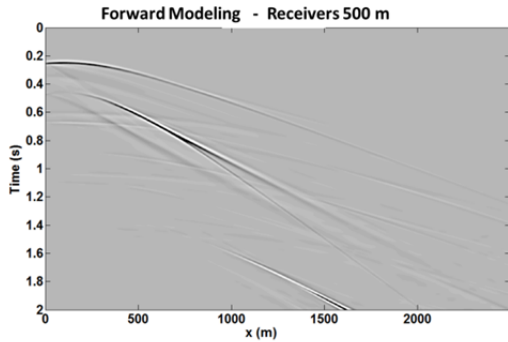


FIG. 4. The source wavefield from modeling: the receivers were located at the position of the interface (500 m depth).

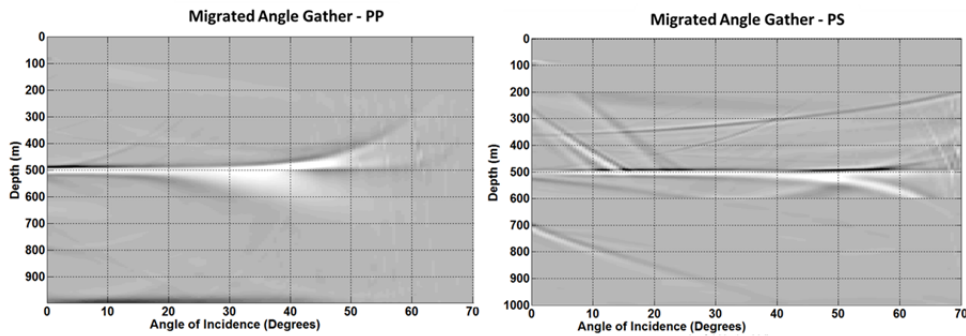


FIG. 5. Migrated data of Model 1 in the angle domain.

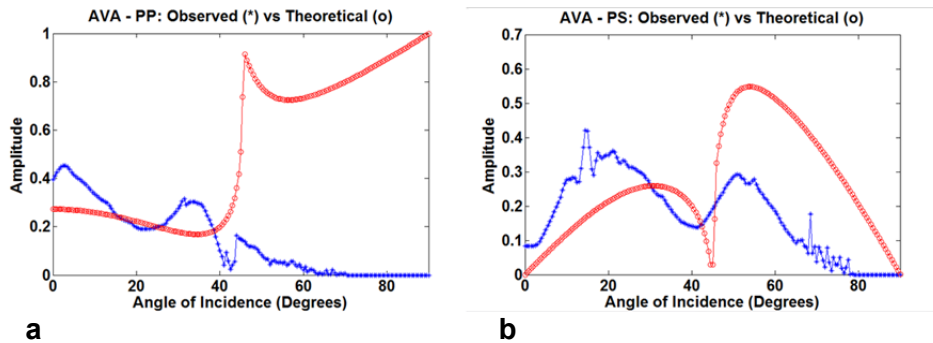


FIG. 6. Comparison of the theoretical Amplitude vs Angle, according to Zoeppritz equations with the amplitudes obtained from migration of Model 1. (a) PP data, (b) PS data.

Figure 7 shows the imaging condition at the depth location of the reflector for Model 2. There are some differences with the result of Model 1, as can be noticed when comparing with Fig. 3(a) and (b): shorter time, and a different pattern of phase variations with offset.

The migrated sections in the angle domain of Figure 8 appear less affected by artifacts than in Model 1, which can be related to a higher critical angle. The amplitude versus angle analysis, Fig. 9, shows a reasonably good agreement of real and theoretical values for angles lesser that the critical angle.

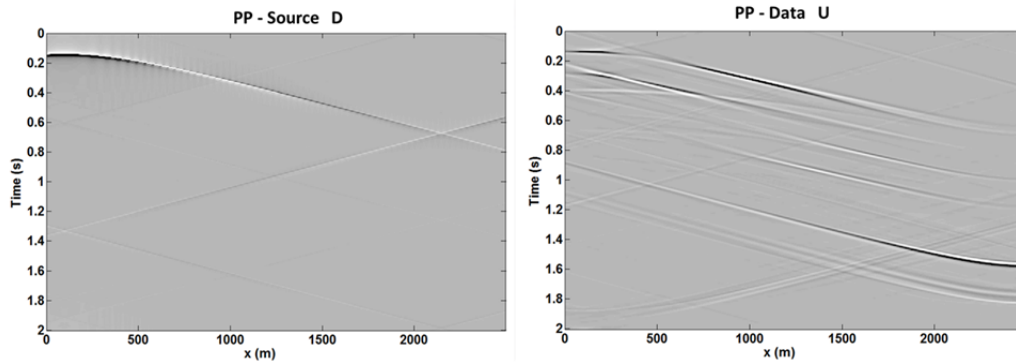


FIG. 7. Downward propagated source (D) and data (U) wavefields for the PP migration of the geological Model 2 at the depth corresponding to the reflector. (a) The source wavefield, (b) the P-wave data (vertical component).

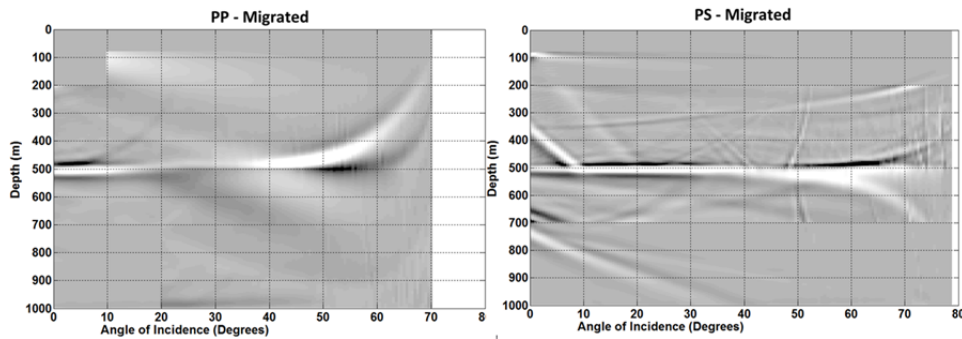


FIG. 8. Migrated data of Model 2 in the angle domain.

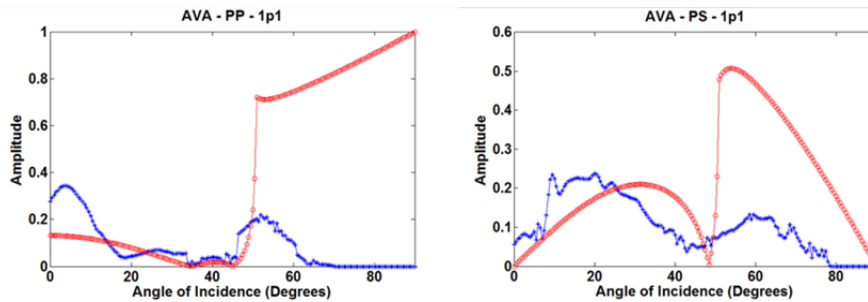


FIG. 9. Comparison of the theoretical Amplitude vs Angle, according to Zoeppritz equations with the amplitudes obtained from a migration of Model 2. (a) PP data, (b) PS data.

DISCUSSION

Modeling was carried out by using a finite difference 2D elastic isotropic code, which has amplitude limitations compared with real data. The source of energy is a shifted Ricker wavelet.

Zoeppritz equations are plane wave solutions, so correspond difference can be expected compared to the modeling result.

Wave mode leakage is apparent in the input data sets, which implies that part of the energy is in both components, especially for larger offsets (i. e. larger angles of incidence).

All these issues can be topics of future research.

CONCLUSIONS

As shown in Figs. 6 and 9, there is a reasonable agreement between the theoretical amplitudes vs. angle as obtained after migration of the synthetic data, for angles lesser than the critical angle, and for PP and PS waves.

There are noticeable differences between the source wavefield as calculated using FD at the reflector location, and the downward propagated source from the Green's functions at the same location, especially related to phase variation with offset.

This is a simple case in ideal condition, so more artifacts and amplitude issues can be expected in real data.

ACKNOWLEDGEMENTS

The financial support of the CREWES sponsors and the technical support of the CREWES staff allowed for the completion of this work.

REFERENCES

- Al-Saleh, S. M., Margrave, G. F., and Gray, S. H., 2009, Direct downward continuation from topography using explicit wavefield extrapolation. *Geophysics*, Vol. 74, No. 6, S105-S112.
- Claerbout, J., 1971, Toward a unified theory of reflector mapping. *Geophysics*, Vol. 36, No. 3, 467-481.
- Ferguson, R. J., and Margrave, G. F., 2005, Planned seismic imaging using explicit one-way operators. *Geophysics*, Vol. 70, No. 5, S101-S109
- Gazdag, J. and Sguazzero, P., 1984, Migration of seismic data by phase shift plus interpolation. *Geophysics*, Vol. 49, 124-131.
- Gray, S., 1997. True amplitude seismic migration: a comparison of three approaches. *Geophysics*, Vol. 63, No. 3, 929-936.
- Margrave, G. F., Ferguson, R. J., and Hogan, C. M., 2010, Full waveform inversion with wave equation migration and well control. CREWES Research Report, V. 22.
- Zhang, Y., Zhang, G, and Bleistein, N., 2005, Theory of true-amplitude one-way wave equations and true-amplitude common-shot migration, *Geophysics*, Vol. 70, No. 4, E1-E10.
- Wapenaar, C. P. A., 1990, Representation of seismic sources in the one-way wave equations. *Geophysics*, Vol. 55, No. 6, 786-790.